Aust. Met. Mag. 44 (1995) 139–145

On computing screen temperatures, humidities and anemometer-height winds in large-scale models

G.D. Hess, R.A. Colman and B.J. McAvaney
Bureau of Meteorology Research Centre, Australia

(Manuscript received August 1994; revised January 1995)

Many large-scale models use the Louis approximate equations to parametrise boundary-layer transfer processes. In this paper a simple, efficient technique is described to derive screen temperatures and humidities and anemometer-height winds from model variables at the surface and the lowest model level. The method uses Dyer-Businger profile relationships to predict the wind, potential temperature and specific humidity at screen or anemometer height. The bulk Richardson number is then calculated and corrected values of the wind, potential temperature and specific humidity are calculated using the Louis profile equations. This ensures consistency in the estimates, since the fluxes were obtained from the Louis scheme. The same methodology could be used directly for other boundary-layer schemes based on Richardson number. For very stable conditions the Dyer-Businger scheme may give poor estimates, but the method still works, provided an upper bound is placed on the Richardson number used in the Louis correction. Convergence to less than five per cent for wind, 0.25 per cent for temperature and five per cent for humidity occurs within two corrections.

Introduction

The Louis scheme (Louis, 1979, 1983; Louis et al. 1982) is widely used in land surface parametrisation schemes (Henderson-Sellers et al. 1994) in large-scale models of the atmosphere. Its purpose is to determine the bulk transfer coefficients, and thus the surface fluxes, as a function of thermal stability. In general, large-scale models employing this scheme have coarse vertical resolution near the surface, and the computed winds, temperatures and humidities are not usually available at standard heights (for example, temperatures and humidities are routinely measured at screen height (~1.5 m) and horizontal winds at anemometer height (usually taken as 10 m)). Because of this, published results are often difficult to compare and interpret. For example, published model output for temperature may be at the lowest model level, the surface skin or the first subsoil layer. To solve this problem a number of methods of interpolation have been suggested to obtain values at standard heights (e.g. Louis 1983; Geleyn 1988; Draxler 1990; McIntosh and Hubbert 1992; McGregor et al. 1993), but these methods are sometimes biased. In this paper we develop a simple technique that is efficient and consistent with the Louis formulation. For the wind, we consider only the magnitude of the horizontal wind speed. Turning of the wind below the lowest model level can be estimated from a simple Ekman model (Holtslag and van Westrhenen 1989).

Corresponding author address: Dr G.D. Hess, Bureau of Meteorology Research Centre, GPO Box 1289K, Melbourne, Vic 3001, Australia.

Methodology

The Monin-Obukhov similarity theory provides the basic framework of our understanding of the atmospheric surface layer. Non-dimensional vertical gradients of horizontal wind, U, potential temperature, Θ, and specific humidity, Q, are assumed to be universal functions of a stability parameter, z/L, where z is the height and L is the Obukhov length:

$$\frac{kz}{u_*}\frac{\partial U}{\partial z} = \phi_M\left(\frac{z}{L}\right) \quad \ldots 1$$

$$\frac{kz}{\Theta_*}\frac{\partial \Theta}{\partial z} = \phi_H\left(\frac{z}{L}\right) \quad \ldots 2$$

$$\frac{kz}{Q_*}\frac{\partial Q}{\partial z} = \phi_Q\left(\frac{z}{L}\right) \quad \ldots 3$$

where u_* is the friction velocity ($u_*^2 \equiv \tau_0/\rho$, where τ_0 is the surface shearing stress and ρ the air density), Θ_* the temperature scale ($\Theta_* \equiv -H_0/\rho c_p u_*$, where H_0 is the surface heat flux and c_p the specific heat of air at constant pressure), Q_* the humidity scale ($Q_* \equiv -E_0/\rho u_*$, where E_0 is the surface evaporative flux), $L \equiv u_*^2/\{(kg/\Theta_{0v})[\Theta_*(1+0.61Q_0)+0.61\Theta_0 Q_*]\}$, g the acceleration due to gravity, k the von Kármán constant and Θ_{0v} the surface virtual potential temperature ($\Theta_{0v} \equiv T_0(P_R/P_0)^{R/C_p}(1+0.61Q_0)$, where T_0 is the surface air temperature, P_0 the surface pressure, P_R the reference pressure (1000 hPa) and R the gas constant for air).

Equations 1 to 3 can be integrated with respect to height to obtain the profile relationships:

$$\frac{kU}{u_*} = \ln\left(\frac{z}{z_0}\right) - \Psi_M\left(\frac{z}{L}\right) + \Psi_M\left(\frac{z_0}{L}\right) \equiv \mathcal{F}_M \quad \ldots 4$$

$$\frac{k(\Theta-\Theta_0)}{\Theta_*} = \ln\left(\frac{z}{z_H}\right) - \Psi_H\left(\frac{z}{L}\right) + \Psi_H\left(\frac{z_H}{L}\right) \equiv \mathcal{F}_H \quad \ldots 5$$

$$\frac{k(Q-Q_0)}{Q_*} = \ln\left(\frac{z}{z_Q}\right) - \Psi_Q\left(\frac{z}{L}\right) + \Psi_Q\left(\frac{z_Q}{L}\right) \equiv \mathcal{F}_Q \quad \ldots 6$$

where the gradients ϕ_M, ϕ_Q in Eqn 1 to 3 and thus their integrated counterparts in Eqns 4 to 6, the profile stability functions Ψ_M, Ψ_H and Ψ_Q, have been determined empirically (e.g. Dyer (1974); the Dyer-Businger profile relations). The experimental limits of the validity of the Dyer-Businger relationships are $-2 \leq z/L \leq 1$ (Kaimal and Finnigan 1994, pp. 15–21). The parameters z_0, z_H and z_Q are the surface roughness lengths for momentum, heat and moisture, respectively. The subscript 0 in Eqns 5 and 6 indicates a surface variable. Since L, z_0, z_H, z_Q, u_*, Θ_* are defined at the surface and therefore independent of height, once they are known, Eqns 4 to 6 can be evaluated at any height z.

The flux evaluation technique developed by Louis (1979) and revised by Louis et al. (1982) and Holtslag and Beljaars (1989) attempts to approximate Eqns 1 to 6, but it is based on the stability parameter known as the bulk Richardson number Ri_b instead of z/L, where Ri_b is defined by:

$$Ri_b = \frac{g\Delta z}{\Theta_v}\frac{\Delta\Theta_v}{|\Delta \underline{U}|^2} \quad \ldots 7$$

where $\Delta\Theta_v$ and $\Delta\underline{U}$ are the differences in virtual potential temperature and horizontal wind velocity over the layer considered. The use of Ri_b as the stability parameter is advantageous because the model equations can be solved directly, whereas the use of z/L requires (expensive) iteration.

In Louis's equations the roughness lengths for heat and moisture are assumed to be equal to that for momentum ($z_0 = z_H = z_Q$); this approximation was introduced for simplicity. He defines the bulk transfer coefficients as:

$$C_D = \left(\frac{k}{\ln\frac{z}{z_0}}\right)^2 F_M\left(Ri_b, \frac{z}{z_0}\right) \equiv \left(\frac{u_*}{U}\right)^2 \quad \ldots 8$$

$$C_H = \left(\frac{k}{\ln\frac{z}{z_0}}\right)^2 F_H\left(Ri_b, \frac{z}{z_0}\right) \equiv \left(\frac{\Theta_*}{\Theta-\Theta_0}\right)\left(\frac{u_*}{U}\right) \quad \ldots 9$$

$$C_Q = \left(\frac{k}{\ln\frac{z}{z_0}}\right)^2 F_Q\left(Ri_b, \frac{z}{z_0}\right) \equiv \left(\frac{Q_*}{Q-Q_0}\right)\left(\frac{u_*}{U}\right) \quad \ldots 10$$

Note that Eqns 8 to 10 depend on both the height z and the stability Ri_b (which is height dependent), where U, Θ and Q are defined at the lowest model level.

Equations 8 to 10 can be rewritten as integrated profile equations in the same form as Eqns 4 to 6. If we do this we obtain the Louis profile equations:

$$\frac{kU}{u_*} = \frac{\left(\ln\frac{z}{z_0}\right)}{F_M^{1/2}\left(Ri_b, \frac{z}{z_0}\right)} \quad \ldots 11$$

$$\frac{k(\Theta-\Theta_0)}{\Theta_*} = \frac{\left(\ln\frac{z}{z_0}\right)}{F_H\left(Ri_b, \frac{z}{z_0}\right)} F_M^{1/2}\left(Ri_b, \frac{z}{z_0}\right) \quad \ldots 12$$

$$\frac{k(Q-Q_0)}{Q_*} = \frac{\left(\ln\frac{z}{z_0}\right)}{F_Q\left(Ri_b, \frac{z}{z_0}\right)} F_M^{1/2}\left(Ri_b, \frac{z}{z_0}\right) \quad \ldots 13$$

We plan to evaluate Eqns 11 to 13 at standard heights. To do this we proceed in two steps. First we estimate U, Θ and Q using the Dyer-Businger formulation (the predictor step) and then we determine U, Θ and Q using the Louis formulation (Eqns 11 to 13) (the corrector step). The procedure is as follows:

1. Evaluate the scaling parameters u_*, Θ_* and Q_* from Louis's profile Eqns 11 to 13 using the model output at the lowest model level (indicated below by a subscript $\sigma 1$, where σ is the vertical coordinate ($\equiv P/P_0$) and P_0 the surface pressure) and output at the surface (indicated by a subscript 0). For humidity the relationship $(Q_0 - Q_{\sigma 1}) = D_w(Q_{sat0} - Q_{\sigma 1})$ is employed (as in the BMRC GCM; this is the so-called β-formulation), where D_w is an efficiency factor and the subscript 'sat' indicates the saturated value (an alternative procedure could be employed, the so-called α-formulation; see e.g. Kondo et al. (1990) and Mahfouf and Noilhan (1991)). We used the F_M function as specified in Holtslag and Beljaars (1989) and F_H and F_Q as given in Miller et al. (1992), but other versions could be used.

2. Determine the Obukhov length L from the scaling parameters.
3. Use Eqns 4 to 6 and the Dyer-Businger profile functions given below to predict the approximate values of U at screen height (1.5 m) and the differences in potential temperature and humidity ($\Delta\Theta$ and ΔQ) for the layer between the screen height and the surface. In unstable conditions $\Psi_M(\zeta) = 2\ln(1+x) + \ln(1+x^2) - 2\tan^{-1} x$ and $\Psi_H(\zeta) = \Psi_Q(\zeta) = 2\ln(1+x^2)$; in stable conditions $\Psi_M(\zeta) = \Psi_H(\zeta) = \Psi_Q(\zeta) = -5\zeta$ where $x \equiv (1-16\zeta)^{1/4}$ and $\zeta \equiv z/L$. The expressions for Ψ_M, Ψ_H and Ψ_Q are also evaluated at z_0/L.
4. Compute the value of Ri_b at the screen height, using Eqn 7 and the information from step 3.
5. Calculate the corrected values of U, $\Delta\Theta$ and ΔQ for the layer between the surface and the screen height by employing the Louis profile relationships Eqns 11 to 13.
6. Steps 4 and 5 could be repeated if necessary, using the Louis profile variables just computed. The process is completed when the convergence criteria are satisfied. We used convergence criteria of five per cent for wind, 0.25 per cent for temperature and 5 per cent for humidity.
7. A similar procedure is used to determine the horizontal wind speed at 10 m height.

Accuracy and efficiency

The accuracy of the Louis scheme has been demonstrated in two ways. Louis (1979) compared his analytical results with those for Dyer-Businger for the bulk transfer coefficients for a range of stability and roughness lengths. In unstable conditions the agreement is generally good for all roughness lengths, but for $Ri_b > 0.2$ the two methods diverge. The failure of the Dyer-Businger method at high stabilities will be discussed further below.

In a second test Louis (1979) simulated the diurnal variation of boundary-layer structure for O'Neill, Nebraska, 24–25 August 1953, and compared his predictions with measurements. The overall agreement was quite favourable, in spite of the simplifications he introduced such as maintaining a constant geostrophic wind.

Geleyn (1988, Figs 1–3) gives a comparison of the iterative solution of the Louis equations with an interpolation solution (Louis 1983) and an analytical solution to approximate the Louis equations (Geleyn 1988). What he calls 'ground truth' is the result found using the same formalism as described above, employing a large number of iterations. Louis's interpolation solution is systematically biased. Geleyn's approximate solution is more efficient than ours since it is analytical, but our method is an efficient way to obtain the 'exact' solution because the predictor is based on the Dyer-Businger formulation. In general we found convergence within two corrections. Our method is directly and simply applicable to other stability functions with Ri dependence, whereas Geleyn's method may require adjustment of his approximate ϕ functions to retain good agreement with the 'exact' solution.

Implementation of the scheme in the BMRC general circulation model

In order to investigate the behaviour of the scheme with general circulation model (GCM) output, additional code was inserted into the Bureau of Meteorology Research Centre (BMRC) GCM. This code calculated predicted values of Θ, Q and U at 1.5 m and 10 m (hereafter subscripted as '1.5' and '10') before every model output archive. It also calculated two 'corrected' values of these variables. Note that in stable conditions the factor z/L was restricted to be no greater than one in the predictor calculation. Note also that care was taken that variables such as Θ_v were calculated in a manner consistent with the diagnosed values of all boundary-layer variables during both predictor and corrector phases. The predictor and each of the correctors were then archived in the model history of state as specially available fields. Of course these calculations could also have been performed 'off line' (i.e. from archived model history of State files) after the GCM run was completed, provided that all required fields were present in the archive.

Model and experiments

Details of the BMRC spectral GCM are not important here, save that the surface eddy fluxes are determined by stability-dependent drag and exchange coefficients determined by a Louis scheme, with a 'low-wind' modification for unstable conditions following the formulation of Miller et al. (1992). Description of the model is given by Bourke et al. (1977) and McAvaney et al. (1978). Details of other parametrisations used in the experiments are given in Hart et al. (1990) and McAvaney and Colman (1993). In the present experiments spectral truncation was set at rhomboidal wave 21, and there were nine vertical levels, defined in 'sigma' coordinates, with the lowest located at $\sigma = 0.991$ (approximately 70 m).

Two experiments, each of 45 days duration, were run, with initial model conditions set at 1 January and 1 July, respectively. A further set of shorter (eight day) experiments was also performed. During all runs model outputs were archived every three hours (at the same time as the

performance of the radiation calculation). Full diurnally and seasonally varying radiation forcing was prescribed. In the following discussion, only the January experiments will be presented, although results from the July experiment are in qualitative agreement with the January results (with allowance made for the change in season).

Results and discussion

Figure 1(a) shows a 30-day average (15 January to 13 February) for the potential temperature predictor ($\Theta_{1.5} - \Theta_0$) at 1200 UTC. Figures 1(b) and 1(c) show the changes in magnitude due to the first and second corrections, respectively. The daily fields display very similar patterns and magnitudes to those shown in Fig. 1, although with, of course, some day-to-day variability. Thirty-day means are shown to highlight the mean boundary-layer structure which prevails in the GCM over the period.

A number of features are apparent in Fig. 1. Firstly, the predictor in places gives large negative screen height/surface potential temperature differences (i.e. $\Theta_{1.5} - \Theta_0$). This is particularly evident over the warm sea-surface temperatures of the western boundary currents, and over ocean points adjacent to land or sea-ice points in the northern hemisphere. In July these differences decrease or disappear completely, although small negative differences arise at ocean points to the Antarctic sea-ice edge (not shown). In each case these regions are associated with cold, dry air (from winter continents or sea-ice) passing over relatively warm oceans. Over these regions, large fluxes of sensible and latent heat occur (not shown) due to the unstable boundary layer and the large vertical gradients in temperature and moisture near the surface.

Large areas of positive $\Theta_{1.5} - \Theta_0$ occur, principally over land. The magnitude of the 30-day mean values is everywhere less than 2°C. These stable regions have a strong diurnal dependence, which will be discussed below.

Figures 1(b) and 1(c) show that the first corrections to $\Theta_{1.5}$ are small, and the second corrections smaller again. During the second correction, changes are everywhere less than 0.7°C in the monthly mean (and generally less than 1°C for daily values—not shown). The sign of the corrections also tends to oscillate between predictor and each subsequent correction, particularly over ocean points. The corrections are also largest (as expected) in regions where the predicted difference between $\Theta_{1.5}$ and Θ_0 is largest.

Moisture fields (not shown) also indicate a rapid decrease in the correction terms. Moisture differences ($Q_0 - Q_{1.5}$) are largest over low latitude oceans, although of course magnitudes of

Fig. 1 Thirty-day means (15 January–13 February) for the screen-height (1.5 m) potential temperature differences from the surface (skin) temperature, at 1200 UTC. The means represent averages over eight archives per day. Shown are (a) predictor (contour interval 2.5 K), (b) the first correction (contour interval 0.25 K) and (c) the second correction (contour interval 0.05 K). The shaded areas are positive.

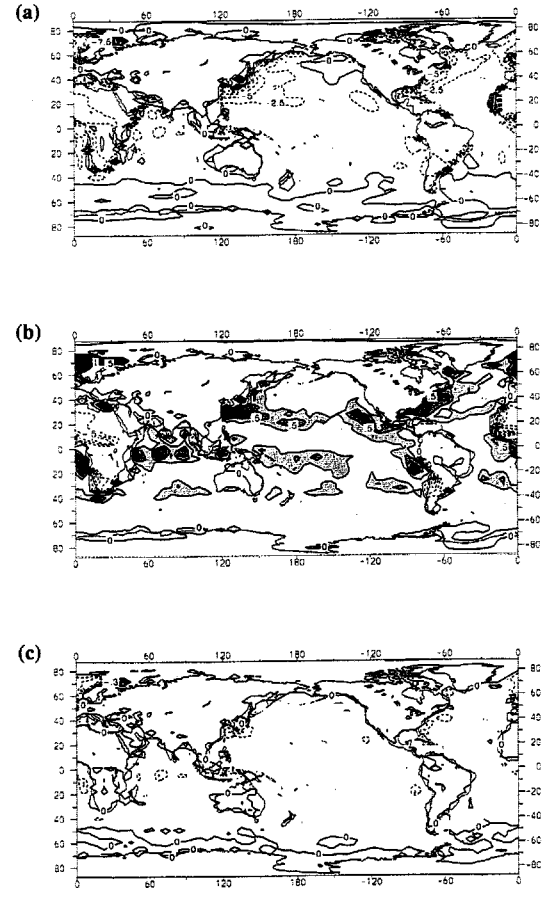

$Q_{1.5}$ are also largest in these regions. In the 30-day mean, second corrections are smaller than 0.5 g kg^{-1} everywhere, with largest values occurring in the subtropics. Once again the sign of the correction tends to oscillate at subsequent correction steps.

Anemometer-height (10 m) wind predictors and first two corrections are shown in Fig. 2. The regions of strongest 10 m winds tend to be (as expected) in the region of the Antarctic circumpolar trough and in the vicinity of the Aleutian and Icelandic lows. The winds also tend to be

Fig. 2 Thirty-day means (15 January–13 February) for anemometer-height (10 m) winds, at 1200 UTC. Shown are (a) predictor (contour interval 2 m s^{-1}), (b) the first correction (contour interval 0.1 m s^{-1}) and (c) the second correction (contour interval 0.05 m s^{-1}).

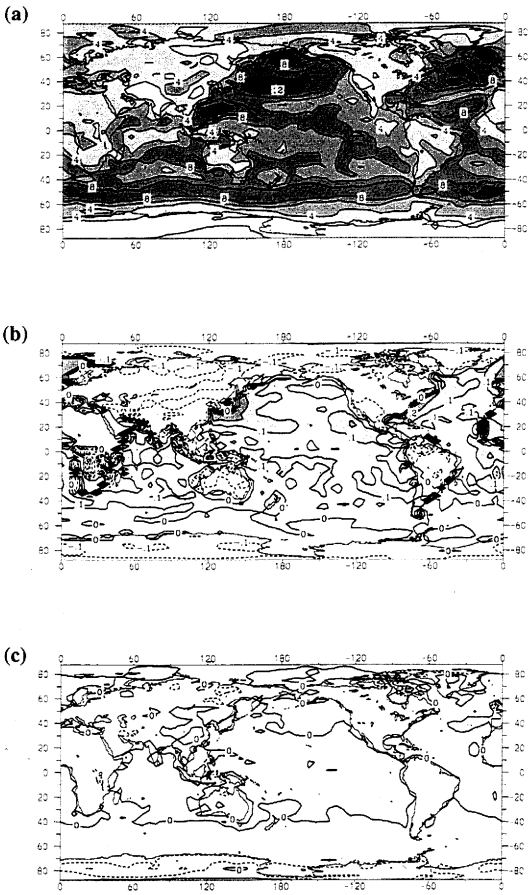

Fig. 3 Screen-height (1.5 m) potential temperature minus the surface potential temperature (30-day mean, diurnal cycle predictor), and the first and second corrections for points selected over (a) eastern Australia (solid line) and the Tasman Sea (dashed line), and (b) the central US (solid line) and over the Kuroshio current (dashed line). Note that in (b) the US curves refer to the left-hand ordinate and the Kuroshio to the right-hand ordinate. A phase shift is present in the curves, because the diurnal cycle at the first model level lags that for the surface temperature. See text for latitude/longitude definitions of the points. The abscissa shows universal (Greenwich) time.

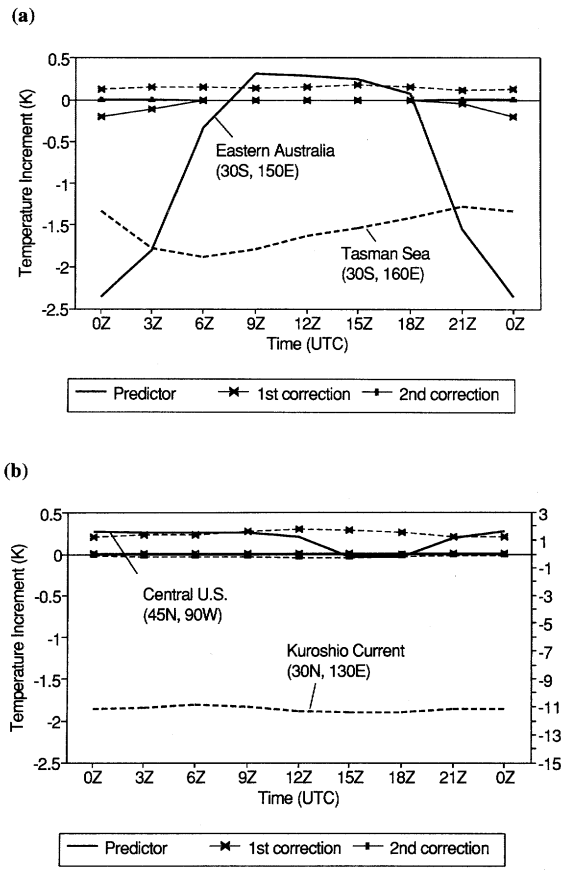

stronger over the ocean than over adjacent land, consistent with the smoother surface (smaller z_0) over the ocean and near-neutral rather than stable (northern hemisphere winter) conditions. Once again, the magnitude of the corrections falls rapidly (to less than 10 cm s^{-1} everywhere by the second correction). However, there is no general 'oscillation of sign' with the correctors, nor do the largest correctors necessarily correspond with the strongest predicted winds. Indeed, the largest correctors tend to be associated with low wind, stable regions. This will be discussed further below.

The mean diurnal cycle of the predictor and subsequent corrections can also be examined from the three-hourly archived values. Only a few select points will be discussed here. These points were chosen to be illustrative, rather than representative. The points selected are at 30°S 160°E (Tasman Sea), 30°S 150°E (eastern Australia), 30°N 130°E (Kuroshio current) and 45°N 90°W (central US). Plots of the diurnal variation of these points are shown in Fig. 3. Once again, 30-day means are shown in order to highlight the mean diurnal cycle.

Over eastern Australia (Fig. 3(a)) a strong diurnal cycle in the predictor is evident. This closely follows the pattern of 1/L (not shown) and reflects the swing from unstable, daytime conditions to stable, night-time conditions which results from the cycle of solar heating and from infrared cooling. The total variation in the mean diurnal cycle is approximately 3°C (of course the total diurnal variation in the surface temperature is much greater than this). Once again the magnitude of the first correction is largest when the predictor is largest in magnitude, but they are of the same sign for this point. The second correction is negligibly small at all times.

For the Tasman Sea point (Fig. 3(a)), a much smaller diurnal range is apparent in the predictor. No night-time stable regime exists here, although during the early morning the boundary layer does become less unstable. The first correction is of opposite sign to the predictor, and remains larger in magnitude than the first correction for the land point, even during those parts of the day in which there are similar-sized predictors. Once again the second correction is negligibly small.

The central US point (Fig. 3(b)) shows a diurnal cycle with a generally stable boundary layer with a brief unstable period during the day. The predictor has a small magnitude, showing a screen-height temperature generally only around 0.25°C warmer than the surface, representing a small, but persistent surface temperature inversion. Sensible and latent heat fluxes (not shown) are small for this point.

The Kuroshio current point (Fig. 3(b)) has a predictor which gives values of $\Theta_{1.5}$ of about 11°C cooler than Θ_0, with extremely small diurnal variation (less than 0.25°C). This reflects the persistence of the outflow of cold lower tropospheric air from the wintertime Siberian high.

These examples serve to illustrate the diurnal and seasonal cycles that are reflected by the boundary-layer temperatures. Similar diagnosis is possible with boundary-layer winds and specific humidity. The point is that the predictor/corrector scheme used here ensures physical consistency between the boundary-layer structure (interpolated winds, temperatures and humidities) and the surface fluxes which occur in the GCM, thereby permitting the performance of such analyses.

Physical consistency of the boundary-layer solution

The Louis scheme gives the integrated profiles from the surface up to the first model level as a function of the bulk Richardson number. To obtain values of U, Θ and Q at intermediate heights, we use the Dyer-Businger profiles which we can implement directly since they depend on z/L rather than Ri_b. These are our best estimates because the Louis scheme was designed to roughly approximate the Dyer-Businger profile relationships. However the procedure can occasionally fail, because of stability limitations of the Dyer-Businger profiles and because of divergence between the two formulations. For example, the Louis scheme yields non-zero turbulent fluxes for $Ri_b > 0.2$, because it is forced to match Ellison's (1957) model as $z/L \to \infty$; the Dyer-Businger scheme yields zero turbulent transfer in this region. For strong stability, dimensional analysis predicts that the profiles should vary linearly with height (e.g. Wyngaard 1973). For extremely stable conditions the turbulence becomes intermittent and the flow becomes decoupled from the surface and is no longer controlled by the surface fluxes. For simplicity we retained the Dyer-Businger scheme for all stabilities.

As a result it is possible, under some atmospheric conditions, for the predictor to produce values of boundary-layer variables which are inconsistent with the surface fluxes. This may be manifest, for example, by values of U_{10} which are larger than the magnitude of the wind at the first model level ($U_{\sigma 1}$), or of $\Theta_{1.5}$ which lie outside the range from Θ_0 to $\Theta_{\sigma 1}$. The removal of such inconsistencies is, of course, the aim of the corrector procedure, which determines the corrections to the boundary-layer profiles which are consistent with the fluxes diagnosed by the Louis scheme. Figures 1 and 2 suggest that they are quickly removed, since the magnitude of the correction required drops off rapidly with subsequent steps. As a test on the operation of this process, a check was made on U_{10} exceeding $U_{\sigma 1}$.

The model was run for eight days with a consistency check performed on all Gaussian grid-points (3584 in number) every time step (64 times per day). Physical inconsistency in the predictor occurred in around 0.25 per cent of all cases, and was associated with light winds and highly stable conditions. As discussed above, for large, positive Richardson numbers wind inconsistencies would be expected between the Dyer-Businger and Louis formulations. Temperature inconsistencies (of up to about 2°C) were also found in about 80 per cent of these very stable, light wind cases. These inconsistencies disappeared after two corrections for U, Θ and Q, providing that an upper bound was placed on the Richardson number. For the Louis stability functions that we employed Ri_b was set to be $\leqslant 20$.

In highly convective conditions the Louis scheme approximates free convection. However, it was found that the differences between the Louis and the Dyer-Businger schemes were unimportant and did not prevent rapid convergence in these circumstances.

Summary

A simple, transparent and efficient method has been developed to obtain winds, potential temperatures and humidities at heights below the lowest model level. The method is physically consistent with the Louis formulation used to determine the surface fluxes. The robust nature of the technique was demonstrated with two experiments, each of 45 days duration, and a set of shorter experiments, each of eight days duration. The merit of the technique is the efficiency provided by good predictors, based on the Dyer-Businger scheme. These estimates are then corrected using the Louis profile equations. In very stable conditions the Dyer-Businger predictor may give poor results, but the method still works, providing that a limit on the Richardson number is imposed. Convergence to less than five per cent for wind, 0.25 per cent for temperature and five per cent for humidity is obtained within two corrections. Another important merit is that the method can be directly applied to other Richardson number boundary-layer schemes.

Acknowledgments

The authors would like to thank Jim Fraser for his assistance with implementing the scheme and with the analysis of the model output, and Terry Hart and Jeff Kepert for critically reading the manuscript. This work was supported by the Department of the Environment, Sport and Territories.

References

Bourke, W., McAvaney, B., Puri, K. and Thurling, R. 1977. Global modelling of atmospheric flow by spectral methods. *Methods in Computational Physics, Vol. 17, General Circulation Models of the Atmosphere*, J. Chang (ed.), New York, Academic Press, 267–324.

Draxler, R.R. 1990. The calculation of low-level winds from the archived data of a regional primitive equation forecast model. *Jnl appl. Met., 29*, 240–8.

Dyer, A.J. 1974. A review of flux-profile relationships. *Bound. Lay. Met., 7*, 363–72.

Ellison, T.H. 1957. Turbulent transport of heat and momentum from an infinite rough plane. *J. Fluid Mech., 2*, 456–66.

Geleyn, J.-F. 1988. Interpolation of wind, temperature and humidity values from model levels to the height of measurement. *Tellus 40A*, 347–51.

Hart, T.L., Bourke, W., McAvaney, B.J., Forgan, B.W. and McGregor, J.L. 1990. Atmospheric general circulation simulations with the BMRC global spectral model: The impact of revised physical parametrizations. *Jnl climate, 3*, 436–59.

Henderson-Sellers, A., Pitman, A.J., Love, P.K., Irannejad, P. and Chen, T. 1994. The project for inter-comparison of landsurface parameterization schemes (PILPS): Phase 2 & 3. *Bull. Am. met. Soc.* (in press).

Holtslag, A.A.M. and Beljaars, A.C.M. 1989. Surface flux parameterization schemes: Developments and experiences at KNMI. *Proceedings Workshop Parameterization of Fluxes over Land Surface*, ECMWF, Reading 24–26 October 1988.

Holtslag, A.A.M. and van Westrhenen, R.M. 1989. Diagnostic derivation of boundary layer parameters from the outputs of atmospheric models. *Scientific Report WR 89-04*, Koninklijk Nederlands Meteorologisch Instituut, de Bilt, The Netherlands.

Kaimal, J.C. and Finnigan, J.J. 1994. *Atmospheric Boundary Layer Flows: Their Structure and Measurement*. Oxford University Press.

Kondo, J., Saigusa, N. and Sato, T. 1990. A parameterization of evaporation from bare soil surfaces. *Jnl appl. Met., 29*, 385–9.

Louis, J.F. 1979. A parameteric model of vertical eddy fluxes in the atmosphere. *Bound. Lay. Met., 17*, 187–202.

Louis, J.F. 1983. Parameterization of sub-grid scale processes. *ECMWF Seminar, 13–17 September 1982, and Workshop, 20–24 September 1982*, ECMWF, Reading, England, 83–97.

Louis, J.F., Tiedtke, M. and Geleyn, J.-F. 1982. A short history of the operational PBL-parameterization at ECMWF. *Workshop on Boundary Layer Parameterization*, 25–27 November 1981, ECMWF, Reading, England, 59–79.

McAvaney, B.J., Bourke, W. and Puri, K. 1978. A global spectral model for simulation of the general circulation. *J. Atmos. Sci., 35*, 1557–83.

McAvaney, B.J. and Colman, R.A. 1993. The AMIP experiment: The BMRC AGCM configuration. *BMRC Research Report No. 38*, Bur. Met., Australia, 43 pp.

McIntosh, P.C. and Hubbert, G.D. 1992. Ocean winds for marine modelling. *Aust. Met. Mag., 40*, 61–9.

Mahfouf, J.F. and Noilhan, J. 1991. Comparative study of various formulations of evaporation from bare soil using in situ data. *Jnl appl. Met., 30*, 1354–65.

Miller, M.J., Beljaars, A.C.M. and Palmer, T.N. 1992. The sensitivity of the ECMWF model to the parametrization of evaporation from the tropical oceans. *Jnl climate, 5*, 418–34.

Wyngaard, J.C. 1973. On surface-layer turbulence. *Workshop on Micrometeorology*, Duane A. Haugen (ed.), Boston, American Meteorological Society, 101–49.